Annu. Rev. Biochem. 2004. 73:241–68
doi: 10.1146/annurev.biochem.73.011303.073626

First published online as a Review in Advance on April 8, 2004

ATP-BINDING CASSETTE TRANSPORTERS IN BACTERIA

Amy L. Davidson[1] and Jue Chen[2]
[1]*Department of Molecular Virology and Microbiology, Baylor College of Medicine, Houston, Texas 77030; email: davidson@bcm.tmc.edu*
[2]*Department of Biological Sciences, Purdue University, West Lafayette, Indiana 47907; email: chenjue@purdue.edu*

Key Words structure, transport, coupling, conformational change, efflux

■ **Abstract** ATP-binding cassette (ABC) transporters couple ATP hydrolysis to the uptake and efflux of solutes across the cell membrane in bacteria and eukaryotic cells. In bacteria, these transporters are important virulence factors because they play roles in nutrient uptake and in secretion of toxins and antimicrobial agents. In humans, many diseases, such as cystic fibrosis, hyperinsulinemia, and macular dystrophy, are traced to defects in ABC transporters. Recent advances in structural determination and functional analysis of bacterial ABC transporters, reviewed herein, have greatly increased our understanding of the molecular mechanism of transport in this transport superfamily.

CONTENTS

INTRODUCTION

Transporters belonging to the ATP-binding cassette (or ABC) superfamily couple the energy released from ATP hydrolysis to the translocation of a wide variety of substances into or out of cells and organelles. The establishment of the family traces its origin to the discovery that a protein responsible for multiple drug resistance in human cancers, alternately referred to as P-glycoprotein, MDR, or ABCB1 (1, 2), bore homology to the well-studied family of periplasmic binding protein-dependent transporters that mediate uptake of a large variety of solutes in gram-negative bacteria (3). P-glycoprotein was later found to reduce the effective concentration of chemotherapeutic drugs inside cells by pumping them out in an ATP-dependent fashion (4). Every ABC transporter appears to be made of four protein domains or subunits: two hydrophobic membrane-spanning domains (MSDs) that are presumed to constitute the translocation pathway or channel across the membrane and two hydrophilic nucleotide-binding domains (NBDs) that interact at the cytoplasmic surface to supply the energy for active transport. The term ATP-binding cassette, which refers to the NBD, was coined to describe the modular nature of these transporters (5); "traffic ATPase" has also been used to describe these transporters because they control the direction of movement of the transported compound (6) in and out of the cells (7).

ABC transporters now constitute one of the largest superfamilies of proteins known (8, 9): There are 48 ABC transporters in humans, and 80 in the gram-negative bacterium *Escherichia coli*. In the transport classification database (10) (http://www-biology.ucsd.edu/~msaier/transport/), the ABC family is currently subdivided into 22 subfamilies of prokaryotic importers, 24 subfamilies of prokaryotic exporters, and 10 subfamilies of eukaryotic proteins. Several other groups maintain online databases, with similar classifications, devoted exclusively to ABC transporters (11, 12). Transporters are assigned to subfamilies on the basis of function and phylogeny, and assignments generally correlate with substrate specificity, though there are exceptions (10, 13, 14). Even though there may be no homology between MSDs in different subfamilies, some degree of homology is maintained across the entire superfamily in the NBDs (25% to 30% identity), suggesting that a similar mechanism for coupling of transport to ATP hydrolysis is employed.

Bacterial Uptake Systems

All bacterial ABC transporters that mediate uptake utilize a high-affinity solute binding protein that is located in the periplasm of gram-negative bacteria and is either tethered to the cell surface (3) or fused to the transporter itself (15) in gram-positive bacteria. These binding protein-dependent transporters take up a wide variety of substrates, which include nutrients and osmoprotectants that range from small sugars, amino acids, and small peptides to metals, anions, iron chelators (siderophores), and vitamin B_{12}. In gram-negative organisms, small substrates gain access to the periplasm via diffusion through outer membrane pore-forming proteins known as porins (16). Larger compounds, such as vitamin

B_{12} and iron-siderophore complexes, are actively transported across the outer membrane through high-affinity transporters utilizing energy transduced from the electrochemical gradient across the cytoplasmic membrane (17).

The high-resolution structures of many periplasmic binding proteins have been determined (18). Three distinct folding patterns have been identified, all of which have two lobes with a substrate-binding site positioned in a cleft between them. The class I and class II binding proteins, represented by the galactose/glucose binding protein and the maltose binding protein, respectively (19), differ primarily in the fold of the two domains. Both classes undergo a conformational change involving the bending of a hinge that joins the two lobes. The binding proteins take on a more open conformation in absence of the transported substrate, and substrate binding promotes bending at the hinge and closing the cleft around the substrate (18, 19). Bound substrates experience rapid exchange, indicating that the two lobes open and close readily even in the presence of substrate (20, 21). Substrate homologues that bind to the binding protein without inducing closure of the substrate-binding cleft may not be transported (21a). Class III binding proteins, represented by the Ferric siderophore binding protein (22) and vitamin B_{12} binding protein (23, 24), have a more rigid hinge structure and may not experience the same type of substrate-induced conformational changes that have been documented in the class I and class II binding proteins.

Binding proteins have two roles in transport; both of which were elucidated from the study of mutant transporters able to function in the absence of a binding protein (25, 26). Although transport still exhibits substrate specificity, the apparent K_m for substrate in the transport reaction is greatly increased in binding protein-independent mutants, indicating that binding proteins are responsible for the high-affinity transport that is characteristic of these transporters. The K_d for substrate-binding to the binding protein often dictates the K_m for substrate in the transport reaction (27). The reason why binding proteins are absolutely required in the wild type is that they stimulate the ATPase activity of the transporters (28, 29). The binding protein-independent mutants display substantially increased rates of ATPase activity as compared to the wild type in the absence of binding protein; this explains how they are able to transport maltose in the absence of binding protein (28, 30).

Further insight into the mechanism of translocation arose from the observation that the maltose binding protein (MBP), which normally displays a low affinity for the maltose transporter ($MalFGK_2$) as judged by the K_m for MBP in the transport reaction (25–100 μM) (31, 32), becomes tightly bound to the transporter in an intermediate conformation stabilized by the phosphate analogue vanadate (33). Following ATP hydrolysis, vanadate becomes trapped along with ADP in one of the two nucleotide binding sites in a conformation that is presumed to mimic the transition state of ATP hydrolysis (34, 36, 37). A trigonal bipyramidal coordination for vanadate, characteristic of the γ-phosphate in the transition state, is seen in the high-resolution structure of vanadate-ADP-inhibited myosin (35). The presence of high-affinity binding between MBP and

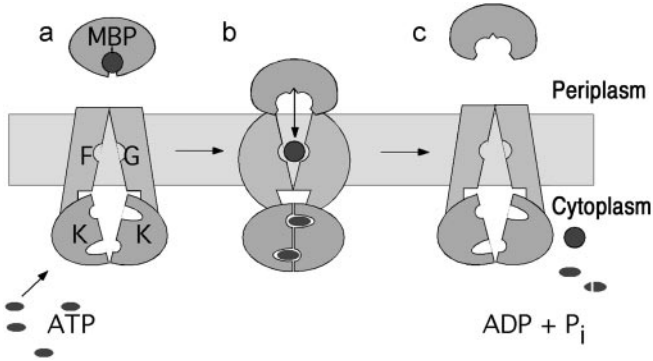

Figure 1 Model for maltose transport. (*a*) MBP, in a closed conformation with maltose bound, interacts with the transporter to initiate transport and hydrolysis. (*b*) In the presumed transition state for ATP hydrolysis, MBP is tightly bound to the transporter in an open conformation that has a lower affinity for maltose, and the transmembrane helices have reoriented to expose an internal sugar-binding site to the periplasm. (*c*) Following ATP hydrolysis, maltose is transported, and MBP is released as the transporter returns to its original conformation. MBP activates the ATPase activity of the transporter by bringing the two NBDs into close proximity, completing the nucleotide-binding sites at the dimer interface. Modified from (33, 90).

$MalFGK_2$ in the presence of vanadate suggests that MBP stimulates the ATPase activity of $MalFGK_2$ by stabilizing the transition state for ATP hydrolysis (33). MBP, trapped in a complex with $MalFGK_2$, no longer binds maltose with high affinity (33), suggesting that it may be open when tightly bound and promote release of maltose into the transmembrane translocation pathway (Figure 1).

Bacterial Efflux Systems

ABC transporters also function in efflux of substances from bacteria, which include surface components of the bacterial cell (such as capsular polysaccharides, lipopolysaccharides, and techoic acid), proteins involved in bacterial pathogenesis (such as hemolysin, heme-binding protein, and alkaline protease), peptide antibiotics, heme, drugs and siderophores (12). Often, the MSD will be fused to the NBD in the bacterial exporters, and two of these half-transporters will interact to complete the four-domain structure of the ABC transporter (38).

In gram-negative organisms, ABC transporters can mediate secretion of their protein substrates across both membranes simultaneously, bypassing the periplasmic space (39). This secretion pathway is referred to as type I secretion and involves two additional accessory proteins in addition to the ABC transporter (6, 39–41). For example, in the secretion of hemolysin (HlyA) from *E. coli*, the inner membrane ABC transporter HlyB interacts with an inner membrane fusion

protein HlyD (42) and an outer membrane facilitator TolC (43). The structure of TolC reveals it is a channel that spans both the outer membrane and the periplasmic space of *E. coli* (44, 45). One domain forms a β-barrel typical of other outer membrane channels, and a second helical domain forms a long narrow cylinder that reaches 100 Å into the periplasm. Although the structure of a HlyD homologue has not been determined, these proteins clearly facilitate the contact between the inner membrane ABC transporter and the TolC channel (46, 47) and may even form part of the *trans*-periplasmic tunnel (48). Translocation through the type I system begins with recognition of the substrate via type I-specific signal sequences in the protein (49–53). Both the MSD and NBD of HlyB have been implicated in substrate recognition (53, 54) as well as in the cytoplasmic domain of HlyD (47). Following recognition, the ABC transporter HlyB presumably transports the unfolded protein across the inner membrane (55–58) and into the attached tunnel where folding might commence (48). The association of inner membrane transporter and outer membrane tunnel appears to be transient, triggered by the binding of substrate to the transport apparatus (46, 47, 59, 60). Transport through inner and outer membrane is tightly coupled; in the absence of TolC, the substrate remains in the cytoplasm rather than being released into the periplasm (61).

ABC proteins that are 35% identical to the mammalian multidrug efflux pump P-glycoprotein are present in bacteria (62, 63). The region of homology extends throughout both the MSD and NBD, suggesting that these ABC proteins may recognize and extrude similar substrates. One such protein, LmrA from *Lactococcus lactis*, has been categorized as a multidrug efflux pump. LmrA mimics the human multidrug resistance phenotype when expressed in lung fibroblasts (62), and expression of LmrA in *E. coli* cells lacking an endogenous multidrug efflux pump increases the resistance of the mutant cell to a large variety of antimicrobial agents (64). Another protein, MsbA from *E. coli*, essential for cell viability, has been categorized as a lipid exporter or lipid flippase (63, 65). At nonpermissive temperatures, cells with a temperature-sensitive mutation in *msbA* fail to translocate newly synthesized phospholipids and lipid A molecules from the inner leaflet of the inner membrane to either the outer leaflet or the outer membrane (66). Though it was originally thought that MsbA transported only lipids (67), purified MsbA can catalyze efflux of fluorescent drug analogues from reconstituted membrane vesicles (68) in keeping with its homology to LmrA and P-glycoprotein. Intriguingly, the *lmrA* gene is able to complement the temperature-sensitive allele of *msbA*, indicating that the physiologic function of LmrA, like MsbA, may be to flip lipids across the bilayer (68). Although it has been known for many years that drug-efflux pumps can contribute to multiple-antibiotic resistance of bacteria (69), most of these drug-efflux pumps are coupled to the proton motive force, and it is not clear whether any ABC transporters contribute to clinically significant multiple-antibiotic resistance in bacterial pathogens (70).

The drug-binding site or sites in P-glycoprotein have been localized to the MSD (71) and display a broad specificity for their mostly hydrophobic substrates. Insight into a mechanism by which these binding sites might accommodate different types of substrates has come from the structures of BmrR and QacR, transcriptional regulators involved in multidrug resistance (72, 73), and from AcrB, a non-ABC efflux pump (74, 75). Drugs with different structures interact with different residues within a large, flexible binding site. Experiments using fluorescent drug analogues in both LmrA and the mammalian P-glycoprotein suggest that these hydrophobic substrates are recruited to the drug-binding site from the inner leaflet of the membrane, where their concentration may be higher than in the cytosol, and released into the aqueous milieu (76, 76a). Alternatively, a lipid flippase would be expected to bind lipids from the inner leaflet and release into the outer leaflet of the membrane (77, 77a). In either case, cycles of ATP hydrolysis are proposed to be coupled to changes in the binding affinity and orientation (high-affinity-inward-facing versus low-affinity-outward-facing) of the drug-binding site(s) within the membrane (34, 78). The Lol transporter in *E. coli* represents an interesting variant of an efflux pump in which the substrates, lipoproteins destined for the outer membrane, are removed from the outer leaflet of the inner membrane and transferred to a periplasmic chaperone for translocation to the outer membrane (79).

In the past five years, several high-resolution structures of ABC transporters, primarily of bacterial or archael origin, have been determined. The focus of this review is to describe the recent insights into the mechanism of translocation and, in particular, ATP hydrolysis and energy coupling, which have been gained from these structures of isolated NBDs and the first intact transporters.

STRUCTURE OF THE ATP-BINDING CASSETTE

A Conserved Structure for Nucleotide-Binding Domains

ABC transporters have two NBDs or nucleotide-binding subunits, also known as ATP-binding cassettes, which power the transporter by binding and hydrolyzing ATP. Presumably, ATP binding and/or hydrolysis are coupled to conformational changes in the MSDs that mediate the unidirectional pumping of substrates across the membrane. Despite the large diversity of the transport substrates, the sequences of the ABC components are remarkably conserved among all ABC

Figure 2 Sequence alignment of all ABC ATPases whose structures have been determined. Sequences are ordered based on their homology to E.c.MalK. Critical conserved sequence motifs are highlighted. Secondary structure elements for E.c.MalK are shown above the sequence. The color schemes for the secondary structure as well as the conserved motifs are the same as in Figure 3.

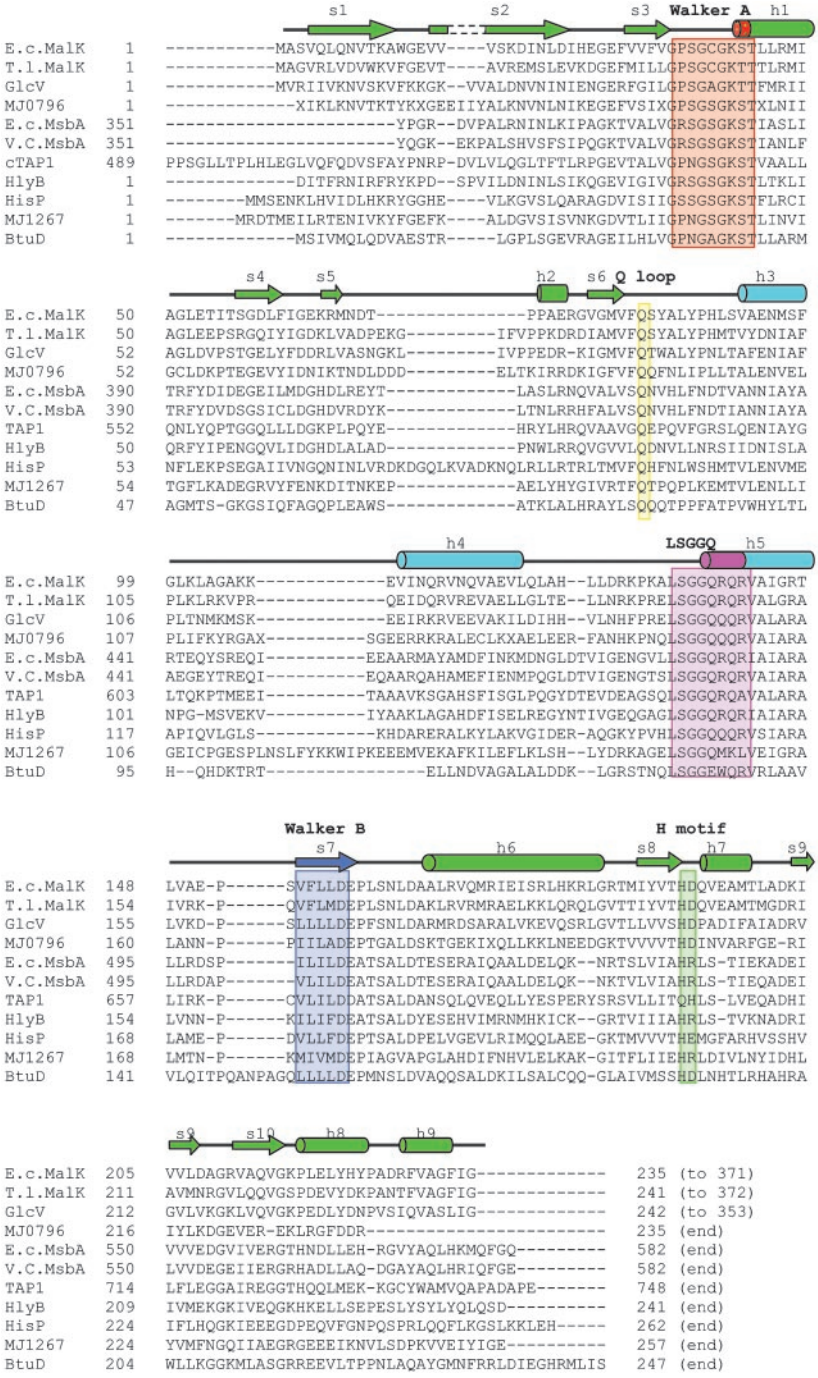

transporters (Figure 2). Several conserved sequence motifs, such as the Walker A and Walker B motifs that are found in many ATPases (80), can be identified, and mutations in these regions often severely reduce or eliminate transport and ATPase activity (70, 81).

The structures of isolated NBDs from eight different transporters, which include both importers (HisP, GlcV, MJ1267, *E. coli* [E.c.MalK], *T. litoralis* [T.l.MalK]) and exporters (TAP, HlyB, MJ0796), have been reported (82–90). The structures, like the sequences, are very similar, and no clear distinction can be made between importer and exporter proteins. The structure of a NBD monomer can be divided into two subdomains (Figure 3*a*): a larger RecA-like (91) subdomain (colored green in Figures 2 and 3) consisting of two β-sheets and six α-helices and a smaller helical subdomain formed by three to four α-helices (colored cyan in Figures 2 and 3). The helical subdomain is specific to the ABC transporters and not seen in other ATPases. ATP is shown bound to the RecA-like subdomain, and the γ-phosphate is positioned close to the edge of one of the β-sheets where it interacts with several residues directly or via H_2O. The Walker A motif, also known as the P loop, follows β-strand 3 and forms a loop that binds to the phosphates of ATP or ADP (Figure 3 and Table 1). The Walker B motif forms β-strand 7, and the terminal aspartate coordinates the Mg^{2+} ion in the nucleotide-binding site through H_2O (85, 86, 89). A glutamate residue immediately following the Walker B binds to the attacking water and the Mg^{2+} ion (87, 92). This glutamate may be the catalytic base for hydrolysis because its mutation leads to complete inactivation of ATPase activity (87, 92). The Q loop, following β-strand 6, also known as the lid (83) or the γ-phosphate switch (85), contains a glutamine that binds to the Mg^{2+} ion and attacking water (87, 89). The structure of the Q loop, which joins the RecA-like subdomain to the helical subdomain, appears to be highly flexible, as reflected by high-B factors in most NBD structures. The flexibility of the Q loop may have an important implication in its function to couple hydrolysis to transport; this function will be discussed below. The H motif following β-strand 8, which has also been referred to as a switch (83), contains a highly conserved histidine residue that forms a hydrogen bond with the γ-phosphate of ATP (87, 90). The signature motif, also known as

Figure 3 Structure of the NBD (residues 1–235) of E.c.MalK with bound ATP (90). (*a*) Stereo view of the monomer. (*b*) The homodimer, consisting of molecules A and B, viewed down the local twofold axis. The RecA-like subdomain is green, and the helical subdomain is cyan. Different colors further distinguish the conserved segments: Walker A motif (*red*), LSGGQ motif (*magenta*), Walker B motif (*blue*), and the Q loop (*yellow*). The ATP is represented in ball-and-stick model [O atom (*red*), N atom (*blue*)]. The color schemes for the domains of the B molecule are similar to those of the A molecule, except that they are rendered in lighter hue. (*c*) Schematic diagram of the interaction between one of the two ATPs bound to the homodimer. Black lines represent van der Waals contacts, and blue lines correspond to hydrogen bonds and salt bridges. Panel *c* reproduced from (90).

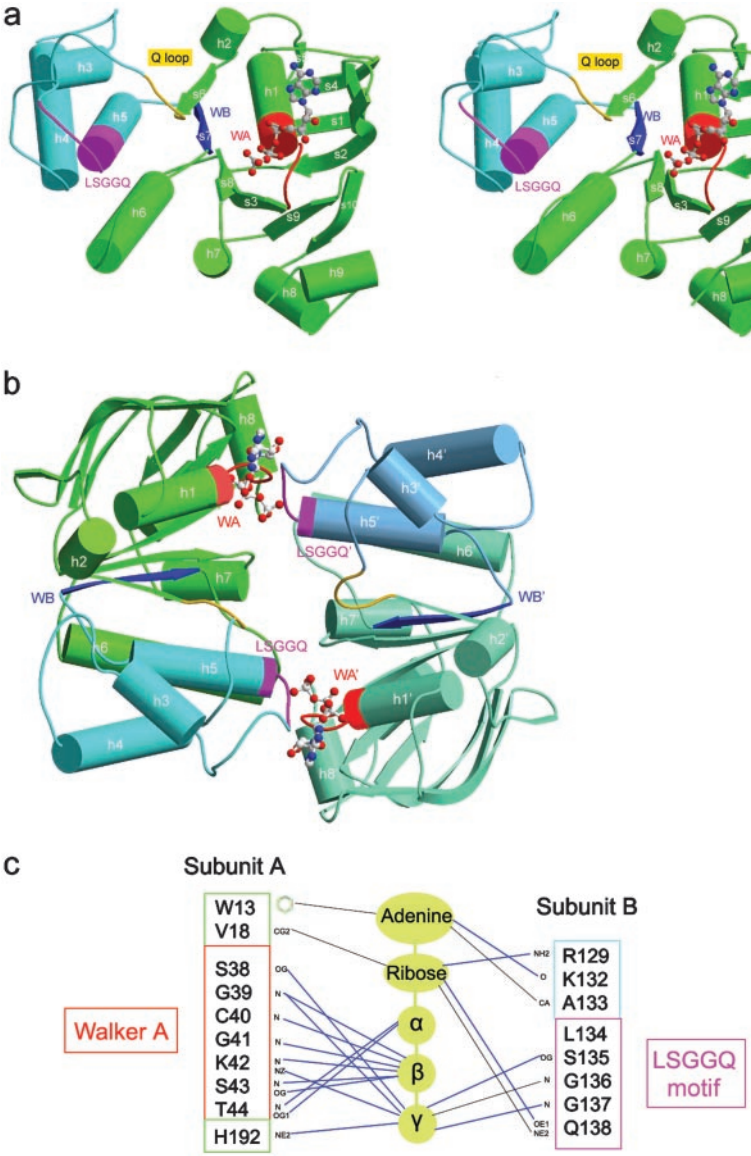

TABLE 1 Function of conserved motifs in the nucleotide-binding domain

Motif	Consensus sequence	Function	Supporting structures[a]
Walker A or P loop	GxxGxGKST[b]	ATP binding	HisP, MJ0796, MJ1267, Rad50, TAP1, GlcV, E.c.MalK
Q loop or lid	Q	a. TM subunit interaction	a. BtuCD
		b. Q H-bond to Mg	b. MJ0796 (E171Q), GlcV/ADP
		c. Binding to the attacking water	c. MJ0796 (E171Q)
LSGGQ or linker peptide or signature motif	LSGGQxQR[b]	ATP binding	Rad50, MJ0796 (E171Q), E.c.MalK
Walker B	hhhhD[b]	D makes a water-bridged contact with Mg^{2+}	GlcV (MgADP, MgAMP-PNP), MJ1267 (MgADP), MJ0796 (MgADP)
	E following Walker B	a. Binds to attacking water	a. MJ0796 (E171Q)
		b. Binds to Mg through a water	b. GlcV (MgADP, MgAMPPNP)
H motif or switch region	H	His H-bond to γ-phosphate	MJ0796 (E171Q), E.c.MalK

[a] References for structures are as follows: HisP (82), MJ0796 (85), MJ1267 (86), Rad50 (99), TAP1 (84), GlcV (89), E.c.MalK (90), BtuCD (105), MJ0796 (E171Q) (87).

[b] Where x represents any amino acid, and h represents a hydrophobic amino acid.

the LSGGQ motif, linker peptide, or C motif, has been used as the "signature" to identify ABC transporters and is the only major conserved motif that does not contact nucleotide in the monomer structure (82). The function of this motif was not clear until the correct dimeric arrangement of ABC proteins was established.

Dimeric Arrangement of Two Nucleotide-Binding Domains in the Transporter

All ABC transporters appear to have two NBDs, and ATP hydrolysis is highly cooperative. This is manifest either by the presence of positive cooperativity in ATP hydrolysis (29, 92, 93) or the loss of function of both nucleotide-binding sites following mutation or modification of a single site (94–97). Based on the structure of the first NBD monomer, HisP (82), and the sequences of atypical ABC transporters that appeared to have only one functional nucleotide-binding

site (98), it was predicted that the NBDs would dimerize with ATP bound along the dimer interface, flanked by the Walker A motif of one subunit and the LSGGQ motif of the other (98). At first, it was not clear whether this was the true interface of the NBDs, because several other ABC crystallographic dimers had been reported (82, 83). Recently, three structures of isolated NBDs have been reported that form a "nucleotide-sandwich" dimer consistent with the predicted structure (98). These include Rad50 (99), an ABC-like ATPase, MJ0796, the NBD subunit of the LolD transporter from *Methanococcus jannaschii* (87), and E.c.MalK, the NBD component of the maltose transporter from *E. coli* (90). In the case of MJ0796, mutation of the catalytic glutamate immediately following the Walker B motif (E171Q) greatly enhanced the stability of the dimer and was necessary to crystallize the protein in this dimeric conformation. As shown for E.c.MalK (Figures 3*b* and 3*c*), residues in the Walker A motif of one subunit and the LSGGQ motif of the other subunit are engaged in extensive interactions with ATP.

Biochemical studies of the intact maltose transporter using vanadate have provided compelling evidence that the ATP-sandwich dimer represents the physiological conformation in the intact transporter. In the presence of UV light, vanadate, which is trapped in the position of the γ-phosphate of ATP (33), mediates highly specific photocleavage of the NBDs at the Walker A and LSGGQ motifs (100). Because the LSGGQ motif is distant from the Walker A motif in a NBD monomer (Figure 3*a*), the close approach of both motifs to the γ-phosphate could occur only across the dimer interface. Hence, the ATP-sandwich dimer appears to resemble the conformation of nucleotide-binding domains in the catalytically active state of the intact transporter when residues from both the Walker A and LSGGQ motifs contact the γ-phosphate.

Elucidation of the correct dimer interface for the NBDs in ABC transporters, together with the observation of nucleotide-dependent association of isolated NBDs (87, 92, 99), has provided answers to several key questions about ABC transporters. First, the functional role of the signature motif is now clearly established. In the dimeric NBD structures, the LSGGQ motif participates in ATP binding and hydrolysis (Figure 3). Second, the dimeric arrangement of the NBDs explains why all ABC transporters have two ABC components. Residues from both subunits are required to form the ATPase active sites, which are located right at the dimer interface. Third, the basis for cooperativity between ATP-binding sites can be explained if both sites must bind ATP before the NBDs can associate into a catalytically active conformation. The structures of MJ0796 (87), E.c.MalK (90), and Rad50 (99) all show two ATP molecules binding symmetrically at the dimer interface, suggesting that two ATPs must bind to form the closed dimer. In the alternating catalytic sites model for hydrolysis as originally proposed by Senior and colleagues (34) for P-glycoprotein, it was hypothesized that ATP binding at one site promoted ATP hydrolysis at the second site. Because only one ADP is trapped by vanadate (36, 37) and it can be trapped in either nucleotide-binding site (101, 101a), it is suggested that only one

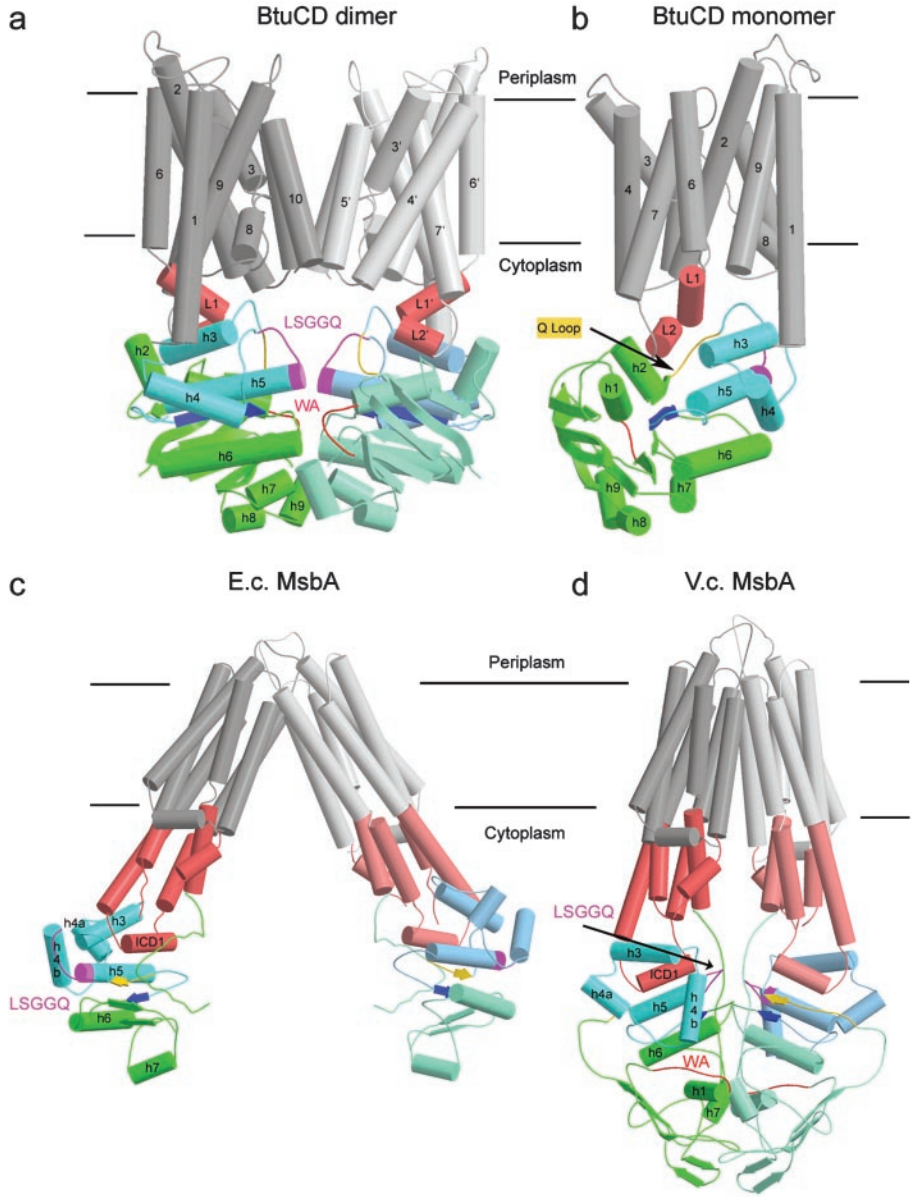

of the two bound ATPs is hydrolyzed per transport event and that the two sites alternate in catalysis (34). It has been difficult to determine whether one or both ATPs are hydrolyzed per transport event. In vivo measurements of growth yields in bacteria suggest that only one ATP is needed to transport one substrate into the cell (102), whereas a recent report using the purified and reconstituted OpuA transporter suggests that two ATPs are needed (103). Models incorporating either one (34) or two ATPs (104) have been proposed.

STRUCTURES OF INTACT TRANSPORTERS

Although the crystal structures of isolated NBDs provide a detailed picture of how these two ATP-binding components interact with each other, the high-resolution structure of an intact bacterial ABC importer should reveal how the NBDs interact with the MSDs and how the MSDs interact with each other. This type of information will form the basis for our understanding of the molecular mechanism by which ATP hydrolysis is coupled to transport. The high-resolution structures of two intact bacterial transporters have been determined: the vitamin B_{12} transporter, BtuCD (105), and the lipid A transporter, MsbA (106, 107).

The Vitamin B_{12} Importer: BtuCD

Vitamin B_{12} is transported into the cell via a periplasmic binding protein-dependent ABC transport system and the transporter itself consists of four subunits, arranged as two homodimers, a transmembrane BtuC dimer, and a nucleotide-binding dimer BtuD. The two BtuC subunits, each consisting of 10 transmembrane α-helices, form a homodimer with a potential translocation pathway located at the interface (Figure 4*a*). This pathway is at least partially accessible to the periplasm and appears closed at the cytoplasm. The two NBDs form a dimer similar to the ATP-sandwich dimer observed in MJ0796 (E171Q) and E.c.MalK (87, 90), except that ATP is absent from the crystal, and the Walker A sequence of one subunit is 4 A° further away from the LSGGQ motif of the opposite subunit. A large cavity is found at the center of the heterotetramer,

Figure 4 Structures of intact ABC transporters. (*a*) Structure of the dimeric vitamin B_{12} transporter BtuCD, front view with the molecular twofold axis running vertically. The MSDs (BtuC) are in gray, and the NBDs (BtuD) are the same colors as in Figure 3. The L loops (L1 and L2) are orange. (*b*) Side view of the BtuCD monomer, 75° from the view in panel *a*, shows docking of the L loop of BtuC into a cleft formed by helices 2, 3 and the Q loop of BtuD. (*c*) Structure of the E.c.MsbA dimer. The MSDs are gray, the ICDs are orange, and the NBDs are cyan and green. The location of the LSGGQ motif is labeled. Most of the RecA-like subdomain, which includes the Walker A motif, is disordered. (*d*) The structure of the V.c.MsbA dimer, colored the same as panel *c*.

below the predicted translocation pathway (Figure 4*a*). This water-filled channel may allow release of substrate into the cytoplasm without disturbing the BtuD dimer (105). The interface between the MSD subunits (BtuC) and the NBD subunits (BtuD) is provided mainly by the cytoplasmic L loop of BtuC and the Q loop on the surface of the BtuD subunit (Figure 4*b*). The L loop forms two short helices connected by a sharp turn (L1 and L2, colored orange in Figure 4*a* and *b*) and docks into a cleft on the surface of BtuD located between the RecA-like subdomain and the helical subdomain (Figure 4*b*). The L loop is likely to correspond to the cytoplasmic loop in other binding protein-dependent MSDs that contain a conserved EAA motif, which has been identified previously as a site of assembly for NBDs on MSDs (107b). Residues around the Q loop that line the cleft in BtuD make extensive contacts with the L1 and L2 helices. Two helices flanking the Q loop, helix 2 of the RecA-like subdomain, and helix 3 of the helical subdomain also make side chain contacts to the L loop of BtuC (Figure 4*b*). Not only is the Q loop a point of contact with the MSDs (105), it is also in contact with atoms in the ATP-binding site (85, 87). Thus, the presence or absence of ATP in the ATPase site has the potential to influence the conformation of the Q loop as well as its interaction with the MSD, thereby providing a pathway for coupling of ATP binding and hydrolysis to rearrangements in the TM region. The Q loop appears to be flexible in most of the ABC structures, perhaps due to the absence of the MSD domain and/or the MgATP. The cleft centered about the Q loop is found on the surface of all isolated NBDs whose structures are known. Hence, the general mechanism of attachment of NBDs to MSDs as well as the mechanism of coupling of transport to hydrolysis may well be conserved throughout the ABC transporter superfamily. In addition to the main contacts between the Q loop and L loop, helix 3 and the following loop also make multiple contacts with the cytoplasmic portion of TM1 in BtuC (Figure 4*a* and *b*). This loop, which connects helix 3 and helix 4, has high sequence and structural variability and may contribute to the specificity needed to prevent cross-reactivity of bacterial NBD subunits with noncognate MSDs (88, 108).

The Lipid A Flippase: MsbA

Two crystal structures of the efflux pump, MsbA, have also been determined, from *E. coli* (E.c.MsbA) (106) and *Vibrio cholera* (V.c.MsbA) (107). MsbA is a half-transporter, meaning that each MSD is fused to a NBD, and two subunits form the functional dimer. Several features of this efflux pump differ from the vitamin B_{12} importer. The six transmembrane helices of the MsbA monomer form a tight bundle (Figure 4*c* and 4*d*), as compared to the more complex architecture of BtuC (Figure 4*a* and *b*). The intracellular loops are generally larger than in BtuC and fold into an intracellular domain (ICD) that extends the transmembrane helical bundle into the cytoplasm (Figure 4*c*). Sequence alignments suggest that ICD may be a general feature for all exporters. In contrast to BtuCD in which the MSD subunits form a tight dimer interface that spans the

membrane (Figure 4*a*), the MSDs of E.c.MsbA are tilted 40° relative to the normal of the membrane and contact each other only in the outer leaflet of the membrane with the effect of spreading the ICD and attached NBDs quite far apart in the cytoplasm in a very open V-shaped configuration (Figure 4*c*). The temperature-sensitive mutation that inactivates E.c.MsbA is located in the MSD dimer interface (66). In V.c.MsbA, which shares 68% sequence identity with E.c.MsbA, the tilt angle is reduced, which causes the transporter to take on a more closed conformation (Figure 4*d*). A patch of positive charge lines a hollow in the interior of the helical bundle in the inner leaflet of the membrane and is proposed as the transport substrate-binding site (106).

The conformation of the NBDs in the two MsbA structures also differs dramatically from that observed in BtuCD and from each other. In E.c.MsbA, the two NBDs are not in contact, and a substantial fraction of the RecA-like subdomain, including the Walker A motif, is disordered (106). The helical subdomain consists of four helices and mediates contact with the ICD. In contrast with BtuCD, where the LSGGQ motif faces into the dimer interface (Figure 4*a*), the LSGGQ motif of E.c.MsbA faces out, away from the twofold axis of symmetry (Figure 4*c*). In V.c.MsbA, the backbone of the entire NBD is resolved in the crystal structure, yet surprisingly, it takes on a conformation not observed in any other NBD to date (107), importer or exporter. In contrast to E.c.MsbA, the helical subdomains of the V.c.MsbA dimer are orientated similarly to those of BtuCD, with the LSGGQ motifs facing toward the dimer interface (Figure 4*d*). However, unlike all other RecA-like subdomains, where 10 β-strands and 6 α-helices pack tightly together, the V.c.MsbA RecA-like domain only consists of 6 β-strands and 3 α-helices. Moreover, there is an unusually large separation between the helical subdomain and the RecA-like subdomain. As a consequence, the dimer contacts observed in BtuCD and other Rad50-like dimers are absent in V.c.MsbA (99), and neither the Walker B motif nor the Q loop is similarly positioned to interact with MgATP as in other structures (Figure 4*d*). This conformation cannot exist in the glucose and maltose importers because the RecA-like subdomain of MsbA would collide with the C-terminal domain of the nucleotide-binding subunits MalK (90, 109) and GlcV (89). At the present time, it remains an open question as to whether the structural differences between BtuCD and MsbA imply different transport mechanisms for uptake and efflux systems, and this question is discussed further below.

CONFORMATIONAL CHANGES IN THE NUCLEOTIDE-BINDING DOMAINS DURING HYDROLYSIS

All of the current models for transport emphasize the key role of protein conformational change in the mechanism by which ATP hydrolysis is coupled to transport. In this section, we summarize the biochemical and structural evidence for conformational changes in the NBDs. Isolated NBDs undergo both an

ATP-dependent association (90, 92) and a γ-phosphate-induced rotation of the helical subdomain relative to the RecA-like subdomain (84, 85), both of which are likely to be an integral part of the mechanism of coupling of transport to ATP hydrolysis.

Evidence of Conformational Change in Nucleotide-Binding Domains

Several lines of evidence indicate that association and dissociation of the NBDs is a key feature of ABC transport. Although the Rad50 protein forms dimers in the presence of ATP (99), ATP-dependent dimerization of isolated transporter NBDs was not observed until the catalytic glutamate was replaced with glutamine (E171Q) in MJ0796 (92). This mutation eliminated hydrolysis and stabilized the ATP-bound dimer. Biochemical evidence in support of the association/dissociation hypothesis also comes from the intact maltose transporter system, in which a fluorescent probe, attached to cysteine 40 in the Walker A motif, becomes less accessible to solvent in the vanadate-trapped, transition state-like intermediate as compared to the ground state (110). Addition of ATP to the intact maltose transporter also enhances disulfide-crosslinking between cysteines introduced at position 85 in the Q loops of the MalK subunits (111). In the structure of E.c.MalK dimer, both of these residues lie along the dimer interface, and the changes are consistent with closure of the dimer interface during ATP hydrolysis (90).

Conformational Changes Revealed by *E. coli* MalK Structures

E.c.MalK is exceptional among NBDs whose structures have been determined because the wild-type protein crystallizes as a dimer in both nucleotide-free and ATP-bound forms (90), making it possible to visualize the MalK dimer in different conformational states. The reason for the increased stability of both the nucleotide-free and nucleotide-bound dimer became clear upon solving the structures. MalK belongs to a group of bacterial sugar transporters that contain an additional C-terminal domain of about 135 residues (3), and subunit-subunit interactions involving the C-terminal domain contribute substantially to the dimer interface (Figure 5). In MalK, this domain, called the regulatory domain, is also known to interact with regulatory proteins, such as enzyme IIA from the glucose-phosphotransferase system (112) and the transcriptional regulator MalT (113, 114). In contrast to the C-terminal domains, which maintain their intersubunit contacts in all of the E.c.MalK homodimer structures, the N-terminal NBDs of E.c.MalK are in close contact only in the ATP-bound structure (Figure 3*b* and 5*a*). In two different nucleotide-free structures that were obtained, the NBDs separated to different degrees (Figure 5*a* and *b*). Hinge bending between the NBD and the regulatory domain is primarily responsible for the separation of NBDs (Figure 5*b*). The motion implied by these structures can be likened to that

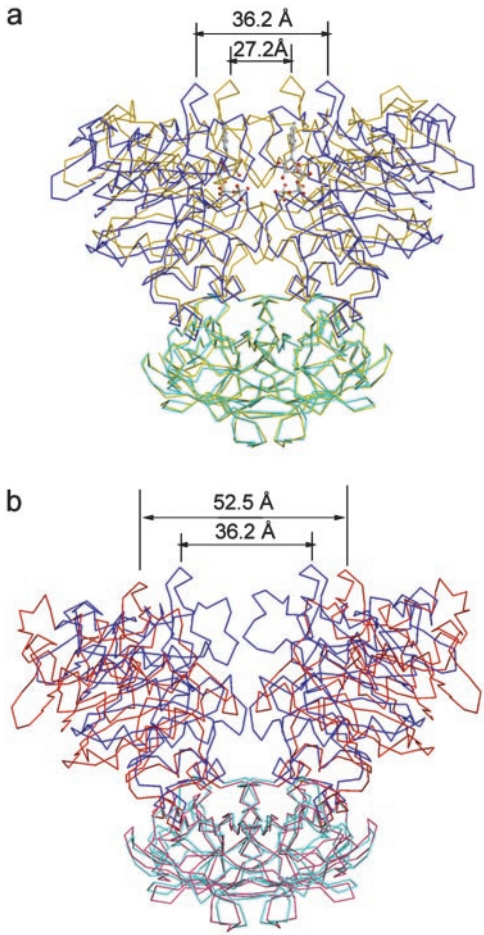

Figure 5 The tweezer-like motion of E.c.MalK dimer. Closed, semiopen, and open structures of E.c.MalK homodimer with superimposed C-terminal regulatory domains. The distances between two H89 residues in a homodimer are indicated. (*a*) Closed form with bound ATP (*yellow*) and semiopen form without bound ATP (*blue*) are superimposed. The excellent overlap of the regulatory domains is evident by the green color, resulting from the combination of yellow and blue colors. (*b*) Superposition of the semiopen (*blue*) and the open (*red*) nucleotide-free structures. Figure is reproduced from (90).

of a pair of tweezers. The regulatory domains represent the handle that holds the two halves together, and the Q loops are positioned at the tips of the tweezers where they can move apart or together. The distance between the two histidines at position 89 in the Q loop increases by either 9 or 25 Å in moving from the closed form to the semiopen or open conformations, respectively (Figure 5*a* and 5*b*). Because the Q loop contacts the MSD of the intact transporter, the motions of the tweezers are likely to induce movements of the MSDs (90).

In addition to the movement of the entire NBDs, MalK also undergoes a hinge rotation of the helical subdomain relative to the RecA-like subdomain. In fact, the relative orientation of the helical subdomain to the RecA-like subdomain varies significantly among all known NBD structures (84, 85). The difference is observed not only in different proteins, but also for the same protein crystallized in different crystal lattices (89, 90), and even between molecules in the same

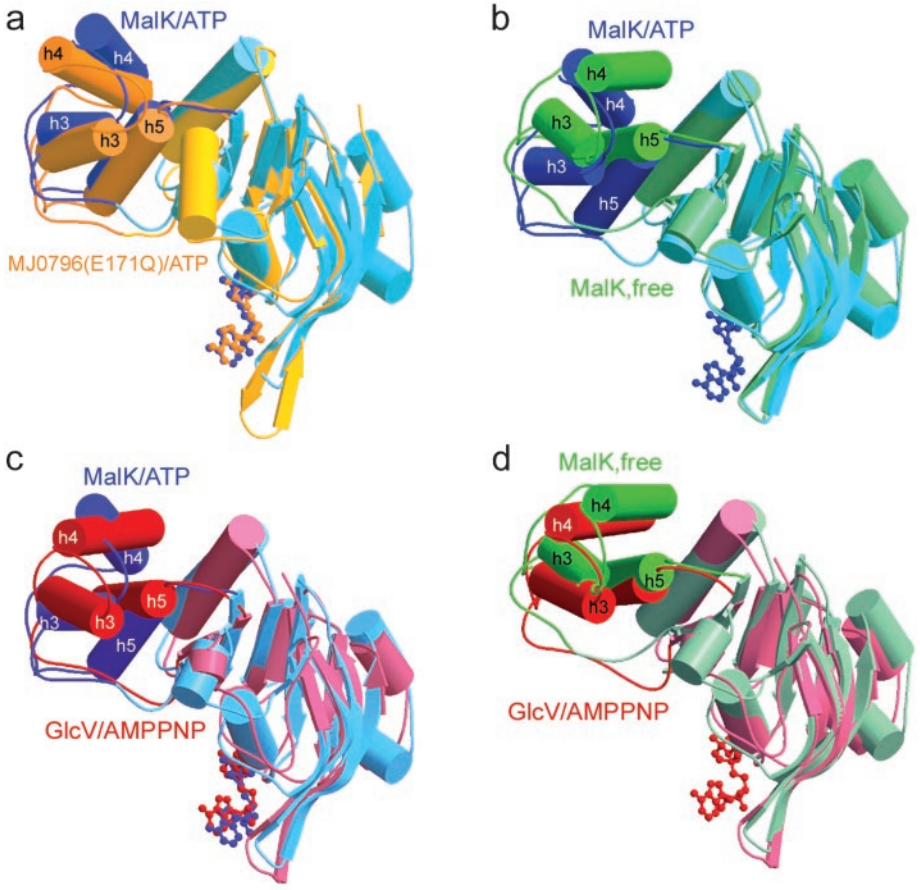

Figure 6 Helical subdomain rotation in NBDs. NBDs are superimposed based on their RecA-like subdomains. The RecA-like subdomains are rendered in lighter color and the helical subdomains in darker color. (*a*) Overlay of two ATP-bound structures: E.c.MalK (*blue*) and MJ0796(E171Q) (*yellow*). (*b*) Overlay of the ATP-bound (*blue*) and the open, nucleotide-free (*green*) E.c.MalK structures. (*c*) Overlay of the ATP-bound E.c.MalK (*blue*) and the AMPPNP-bound GlcV (*red*) structures. (*d*) Overlay of the open, ATP-free E.c.MalK (*green*) and the AMPPNP-bound GlcV (*red*) structures.

crystal lattice (83). The hinge rotation of the helical subdomain relative to the RecA-like subdomain ranges from 5° to 25°, depending on the structures that are compared. However, when the three available ATP-bound structures, HisP, E.c.MalK, and MJ0796(E171Q), are compared, the orientation of the helical subdomains are essentially the same (Figure 6*a* versus Figure 6*b*), indicating that in the presence of the γ-phosphate, the helical subdomain becomes locked into one orientation. Interestingly, the helical subdomain of GlcV in the presence of

the nonhydrolyzable ATP analogue Mg/AMPPNP folds into an orientation more similar to the nucleotide-free than the ATP-bound form of E.c.MalK (Figure 6*c* versus Figure 6*d*), suggesting that AMPPNP is not a good mimic of ATP for ABC transporter proteins. AMPPNP and ATPγS, another nonhydrolyzable analogue, also failed to support dimerization of MJ0796(E171Q) (92). One could argue that the difference in the helical subdomain orientation is simply a crystallographic artifact, i.e., that protein-protein contacts inside a crystal lattice stabilize the helical subdomain in a particular orientation. However, the fact that the flexibility of the helical subdomain was observed only in structures lacking the γ-phosphate of ATP suggests that it has important mechanistic implications. In the context of the isolated NBD, it has been suggested that its function is to withdraw the signature motif, located N-terminal to helix 5, from the ATP binding site in order to facilitate release of ADP following hydrolysis (86). It is clear from structures of ATP-bound dimers that NBDs must dissociate to permit nucleotide binding and release. In the context of the intact transporter, it has been suggested that this hinge rotation is controlled by the MSDs to regulate the ATPase activity of the NBDs (87, 108). When the helical subdomain is rotated away from RecA subdomain, as in the nucleotide-free conformation (Figure 6), the two NBDs cannot approach closely enough to form the ATP-bound dimer. For example, this rotation could be tied to the mechanism by which drug binding to the MSD stimulates ATP hydrolysis by an efflux pump. The added flexibility of this hinge may also be important in adjusting the size of the opening of the translocation pathway to accommodate the size of the substrate.

Comparison of the BtuCD structure (105) to the E.c.MalK dimer structures (90) reveals that the BtuD dimer is very similar to the semiopen MalK configuration. Hence, there appears to be a role for both helical subdomain rotation and NBD closure in proceeding from the open conformation observed in the BtuCD structure to the closed-ATP-bound conformation. This observation also confirms that the conformational changes identified in the isolated MalK dimer are representative of what will occur in the intact transporter complex.

Two Physiological Conformational States for Nucleotide-Binding Domains of MsbA?

As we have discussed, nucleotide-free MsbA from *E. coli* and *V. cholera* crystallized in different conformations, neither of which contains an NBD dimer resembling either the BtuD dimer or the E.c.MalK dimers in their open and closed conformations. Given the good agreement between the BtuCD structure and the E.c.MalK dimer structures, and between these structures and biochemical characterizations of ABC transporters, serious questions have been raised about whether the MsbA structures should be viewed as conformational intermediates in the cycle of an efflux pump or as nonphysiologic conformations introduced during the purification or crystallization of the transporter (115–117). Assuming the two MsbA structures are different physiologic intermediates or snapshots of the catalytic cycle, then the conformational changes required to bring the open

E.c.MsbA conformation (Figure 4*c*) to the closed V.c.MsbA conformation (Figure 4*d*) are quite dramatic. Not only must each MsbA monomer rotate inward ~15° to bring the MSDs and NBDs close together, but the NBDs must also rotate around the ICDs by ~120°. The latter rotation would present the LSGGQ motif in the helical subdomain to the dimer interface as observed in the other NBD dimers. In addition, the author (107) indicates that the RecA-like subdomains of V.c. MsbA would have to swing ~180° toward the helical subdomains to convert the NBD dimer in V.c.MsbA to a dimer resembling BtuD that could bind ATP. Because the NBD of V.c.MsbA contains substantially fewer β-strands and α-helices than most NBDs, significant refolding of the structure would have to occur in order to bring this structure into compliance with the Rad50-like dimer interface.

Translation of this complex series of conformational changes into a plausible mechanism for translocation would, in our opinion, be extremely difficult, whereas the conformational changes demonstrated in the MalK dimer, as discussed in the next section, offer a simple explanation of how transport is coupled to hydrolysis in both importers and exporters in the ABC family.

MECHANISMS FOR COUPLING OF HYDROLYSIS TO TRANSPORT

Models for Coupling in Periplasmic Binding Protein-Dependent Transport

Substantial evidence has accumulated in support of a model in which ATP hydrolysis is coupled to conformational changes in the transporter that mediate the movement of substrate across the membrane. This concept is illustrated in the model for maltose transporter (Figure 1) in which an energetically favorable event (ATP hydrolysis) and an energetically unfavorable event (maltose transport against a concentration gradient) are linked via a common conformational intermediate. This conformation was trapped with vanadate acting as a transition state analogue (33). The concerted conformational changes in MBP and $MalFGK_2$ required to form this intermediate simultaneously promote both ATP hydrolysis and release of maltose from MBP directly into the mouth of the translocation pathway.

From the structure of the binding protein-dependent vitamin B_{12} transporter in a nucleotide-free state, it is now possible to address what type of conformational changes need to occur in transmembrane regions to facilitate transport and how they might be coupled to conformational changes in NBDs. In the nucleotide-free structure of BtuCD, the proposed transmembrane translocation pathway appears to be at least partially open to the periplasm and closed at the cytoplasm (105), suggesting that a cytoplasmic gate must open at some point in the translocation cycle. The authors (105) propose a model in which the closure of the NBDs that

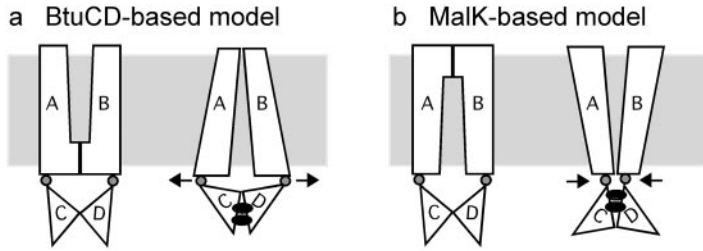

Figure 7 Two models for coupling of NBD closure to transmembrane movement. (*a*) BtuCD-based model. NBD closure coincides with opening of translocation pathway to cytoplasm. (*b*) E.c.MalK-based model. NBD closure coincides with closing of translocation pathway to cytoplasm and opening to periplasm.

accompanies binding and hydrolysis of ATP opens the gate by forcing the MSDs apart in a motion analogous to that of a toggle switch (Figure 7*a*). However, the E.c.MalK dimer structures (Figure 5) suggest that the residues in MalK and BtuD that make contact with the MSDs would be closer together in the ATP-bound form as compared to the free form, making it difficult to understand how closure of NBDs could mediate opening of a cytoplasmic gate in either system. Based on the E.c.MalK structures, a different model is proposed (90) that predicts movement of the MSDs opposite to the movement observed in the BtuCD-based model (Figure 7*b*). In the MalK-based model, the transmembrane pathway is open to the cytoplasmic side in the resting state, and ATP-induced closure of the NBDs mediates the closing of a gate at the cytoplasmic surface of the MSDs and the opening of a gate at the periplasmic surface, thereby alternating access to a central translocation pathway through the membrane. If the model in Figure 7*b* is correct, and it applies equally well to both maltose and B_{12} transport, then the conformation of BtuCD captured in the crystal may be an intermediate between the resting state and the transition state in which the cytoplasmic gate has already closed, but the periplasmic gate has not yet fully opened. The observed flexibility of the hinge between the RecA-like subdomain and the helical subdomain in the NBDs (Figure 6) could permit a more open conformation of BtuCD, which is observed in one of the MalK dimer structures (90). Clearly, more biochemical and structural analyses of intact ABC transporters are needed to clarify the mechanism of translocation.

Models for Coupling in Drug Efflux Systems

Just as maltose is transferred from a high-affinity binding site on one side of the membrane to a low-affinity binding site on the other side (Figure 1), drug transport is suggested to involve changes in drug-binding site affinity and orientation (inward versus outward facing) during a cycle of ATP hydrolysis (78). In the original model for alternating sites, Senior and colleagues (101) noted

that, although ATP does not bind with high affinity to ABC transporters, ATP hydrolysis results in the formation of a high-energy state with ADP and P_i bound and suggests that relaxation of this state (i.e., the release of P_i) might be accompanied by the conformational changes that result in drug transport. They now postulate that both the formation and collapse of the transition state of catalysis are critical events for driving the conformational changes that mediate drug transport (78) as illustrated in our model for maltose transport (Figure 1). Binding of drug substrate, or periplasmic binding protein, promotes the formation of the catalytic transition state by promoting NBD closure, and subsequent ATP hydrolysis leads to NBD dimer reopening. In both drug efflux pumps and bacterial uptake systems, it appears that this closed state can be trapped either with a transition state nucleotide analogue (33, 37) or with ATP if hydrolysis is prevented through mutation of a key catalytic residue (92, 118–120).

Evidence for conformational coupling between nucleotide-binding sites and drug-binding sites in the MSD of drug efflux pumps has come from both vanadate-trapping experiments (37, 121, 122) and spectroscopic studies (123, 124) in prokaryotic and eukaryotic systems. In the bacterial LmrA protein, a combination of infrared spectroscopy and hydrogen/deuterium exchange kinetics was used to show that ATP hydrolysis triggered substantial changes in accessibility of the residues in the TM domain without accompanying changes in mean helix orientation (125), suggesting that helix translation or, in particular, helix rotation could alternately expose the drug-binding site to the lipid environment or to the aqueous extracellular environment (125). Binding of radiolabeled vinblastine to LmrA displays positive cooperativity, although both cooperativity and high-affinity binding are lost in the vanadate-trapped intermediate (122). These data are consistent with the interpretation that drug transport occurs coincidently with ATP hydrolysis, and the authors (122) suggest vanadate has stabilized an intermediate in which the drug-binding site is occluded during the switch from a high-affinity inward-facing state before hydrolysis to a low-affinity outward-facing state after hydrolysis. They propose a variation of the alternating catalytic sites model (34), likened to a two-cylinder engine, in which each half-transporter has its own drug carrier site, and while ATP hydrolysis occurs concomitantly with drug transport in one half of the transporter, the second half resets its drug-binding site from the outward-facing low-affinity conformation to the inward-facing high-affinity conformation (122). This model (Figure 8*a*) can be contrasted to models proposed for the mammalian P-glycoprotein (Figures 8*b* and 8*c*) in which one interchangeable drug-binding site is shared between the two halves of the pump (78) or in which both high- and low-affinity sites coexist, and loss of high-affinity binding in the transition state promotes transfer of drug from the high-affinity (on) site to the low-affinity (off) site (104). Although the first two models incorporate the concept that drug transport occurs each time ATP is hydrolyzed, the authors of the third model suggest that ATP hydrolysis at the second site is required to reset the system before transport can occur again (104). Both key concepts in this final model, the loss of high-affinity binding in the catalytic transition

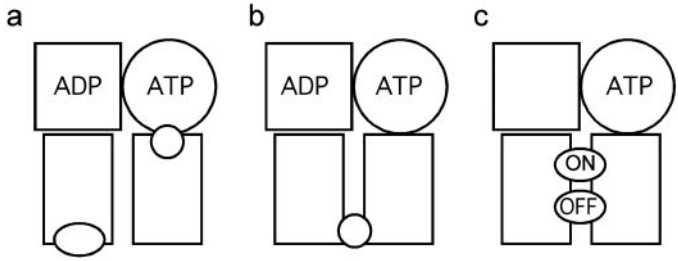

Figure 8 Three models for multidrug efflux pumps. (*a*) Model 1 (122). Each half-transporter has a drug-binding site, and during ATP hydrolysis, one site reorients from inward-facing to outward-facing while the other site reorients from outside to inside. (*b*) Model 2 (34). A single drug-binding site, shared between the MSDs, reorients from inward-facing to outward-facing following ATP hydrolysis. (*c*) Model 3 (104). Two binding sites coexist, an inward-facing (ON) site and an outward-facing (OFF) site. Loss of high-affinity binding to the ON site in the transition state promotes transfer of drug from the ON site to the OFF site.

state and the requirement for ATP hydrolysis in resetting the system, have recently been challenged on the grounds that they rely too heavily on the use of photoaffinity labeling by drugs to assess changes in drug-binding site affinity (126).

Other models for transport by P-glycoprotein have also been proposed. Higgins and colleagues report a lowered drug-binding affinity both in the presence of the nonhydrolyzable ATP analogue AMPPNP and in the vanadate-trapped transporter (127). Medium resolution structures of P-glycoprotein obtained by cryo-electron microscopy of two-dimensional crystals provide evidence for at least three distinct arrangements for the MSDs (128). Crystals of P-glycoprotein formed in the presence of AMPPNP differ from those obtained in the absence of nucleotide, and the vanadate-trapped species adopts a third conformation. On the basis of these observations, the authors suggest that nucleotide binding to P-glycoprotein rather than ATP hydrolysis drives the major conformational changes that reorient the drug-binding site from the inside to the outside of the cell (127). Consistent with this hypothesis, nonhydrolyzable nucleotide analogues or ATP in the absence of Mg will support opening of the mammalian cystic fibrosis transmembrane regulator channel (129).

A recent study based upon thermodynamic analysis of the intrinsic rate-limiting step of drug transport indicates that P-glycoprotein undergoes two distinct catalytic cycles in the presence and absence of drug with different rate-limiting transition states (130). In an extension of the alternating catalytic sites model (34), the authors propose (130) that drug is still bound at a high-affinity site in the drug-coupled transition state because the catalytic constant for ATP hydrolysis varies with different drugs. They also postulate that during ATP hydrolysis in the absence of drug, the drug-binding site is in the low-affinity form (130). This latter postulate clearly complicates interpretation of published vanadate-trapping experiments if, in fact, vanadate traps a conforma-

tion of the transporter seen only in the basal transition state and not in the drug-coupled transition state.

CONCLUDING REMARKS

Great advances have been made in the past several years in our understanding of the molecular mechanism of translocation in bacterial ABC transporters. Both biochemistry and structural biology have had equally important roles in these advances. As we have discussed, the progress in structural biology has been mired by seemingly contradictory results, and only by interpreting the structures based on the results of biochemical analyses and determining what is and is not plausible has it been possible to put together a reasonable model of the way transport occurs. Stabilization of conformational intermediates in the transport cycle, in particular through the use of vanadate, has been key to the advances made in biochemical characterization of ABC transporters, and it is hoped that crystal structures of these conformational intermediates alongside their ground state counterparts will further the field.

Although most of the recent progress in structural biology has been made with prokaryotic family members, it is likely that eukaryotic transporters will utilize the same mechanisms for translocation. The structure of TAP1, the NBD of the mammalian transporter involved in antigen processing, has been determined, and it is essentially the same as that seen in the prokaryotic NBD structures (84). Defects in many of the human ABC transporters have been linked to disease, and many of their physiologic functions have been deduced (9). It is hoped that, through the study of bacterial homologues, we will come to a better understanding of the structure, function, and mechanism of human protein action.

ACKNOWLEDGMENTS

Work in the Davidson lab was supported by grants from NIH (R01 GM49261) and the Welch Foundation (Q-1391). Work in the Chen lab was supported by the Pew Scholarship and an American Cancer Society Institutional Research Grant to the Purdue Cancer Center. We thank James Westbrooks, Kimberly Westbrooks, and Tasha Biesinger for their comments on the manuscript.

The *Annual Review of Biochemistry* is online at http://biochem.annualreviews.org

LITERATURE CITED

1. Chen C-J, Chin JE, Ueda K, Clark DP, Pastan I, et al. 1986. *Cell* 47:381–89
2. Gros P, Croop J, Housman D. 1986. *Cell* 47:371–80
3. Boos W, Lucht JM. 1996. In Escherichia coli and Salmonella: *Cellular and Molecular Biology*, ed. FC Neidhardt, R Curtiss III, JL Ingraham, ECC

Lin, KB Low, et al. pp. 1175–209. Washington, DC: ASM Press
4. Horio M, Gottesman MM, Pastan I. 1988. *Proc. Natl. Acad. Sci. USA* 85:3580–84
5. Hyde SC, Emsley P, Hartshorn MJ, Mimmack MM, Gileadi U, et al. 1990. *Nature* 346:362–65
6. Holland IB, Blight MA. 1999. *J. Mol. Biol.* 293:381–99
7. Ames GFL, Mimura CS, Shyamala V. 1990. *FEMS Microbiol. Rev.* 6:429–46
8. Dassa E, Hofnung M, Paulsen IT, Saier MH Jr. 1999. *Mol. Microbiol.* 32:887–89
9. Dean M, Hamon Y, Chimini G. 2001. *J. Lipid Res.* 42:1007–17
10. Saier MH Jr. 2000. *Microbiol. Mol. Biol. Rev.* 64:354–411
11. Quentin Y, Fichant G. 2000. *J. Mol. Microbiol. Biotechnol.* 2:501–4
12. Dassa E, Bouige P. 2001. *Res. Microbiol.* 152:211–29
13. Saurin W, Dassa E. 1994. *Protein Sci.* 3:325–44
14. Kuan G, Dassa E, Saurin W, Hofnung M, Saier MH. 1995. *Res. Microbiol.* 146:271–78
15. van der Heide T, Poolman B. 2002. *EMBO Rep.* 3:938–43
16. Delcour AH. 2003. *Front. Biosci.* 8:d1055–71
17. Postle K, Kadner RJ. 2003. *Mol. Microbiol.* 49:869–82
18. Quiocho FA, Ledvina PS. 1996. *Mol. Microbiol.* 20:17–25
19. Wilkinson AJ, Verschueren KHG. 2003. In *ABC Proteins: From Bacteria to Man*, ed. IB Holland, SPC Cole, K Kuchler, CF Higgins, pp. 187–207. London: Academic
20. Miller DM, Olson JS, Pflugrath JW, Quiocho FA. 1983. *J. Biol. Chem.* 258: 13665–72
21. Ledvina PS, Tsai AL, Wang Z, Koehl E, Quiocho FA. 1998. *Protein Sci.* 7:2550–59
21a. Hall JA, Thorgeirsson TE, Liu J, Shin YK, Nikaido H. 1997. *J. Biol. Chem.* 272:17610–14
22. Clarke TE, Ku SY, Dougan DR, Vogel HJ, Tari LW. 2000. *Nat. Struct. Biol.* 7:287–91
23. Borths EL, Locher KP, Lee AT, Rees DC. 2002. *Proc. Natl. Acad. Sci. USA* 99:16642–47
24. Karpowich NK, Huang HH, Smith PC, Hunt JF. 2003. *J. Biol. Chem.* 278: 8429–34
25. Treptow NA, Shuman HA. 1985. *J. Bacteriol.* 163:654–60
26. Ames GFL, Mimura CS, Holbrook SR, Shyamala V. 1992. *Adv. Enzymol. Relat. Areas Mol. Biol.* 65:1–47
27. Merino G, Boos W, Shuman HA, Bohl E. 1995. *J. Theor. Biol.* 177:171–79
28. Davidson AL, Shuman HA, Nikaido H. 1992. *Proc. Natl. Acad. Sci. USA* 89:2360–64
29. Liu CE, Liu PQ, Ames GFL. 1997. *J. Biol. Chem.* 272:21883–91
30. Petronilli V, Ames GFL. 1991. *J. Biol. Chem.* 266:16293–96
31. Manson MD, Boos W, Bassford PJ Jr, Rasmussen BA. 1985. *J. Biol. Chem.* 260:9727–33
32. Dean DA, Hor LI, Shuman HA, Nikaido H. 1992. *Mol. Microbiol.* 6:2033–40
33. Chen J, Sharma S, Quiocho FA, Davidson AL. 2001. *Proc. Natl. Acad. Sci. USA* 98:1525–30
34. Senior AE, Al-Shawi MK, Urbatsch IL. 1995. *FEBS Lett.* 377:285–89
35. Smith CA, Rayment I. 1996. *Biochemistry* 35:5404–17
36. Sharma S, Davidson AL. 2000. *J. Bacteriol.* 182:6570–76
37. Urbatsch IL, Sankaran B, Weber J, Senior AE. 1995. *J. Biol. Chem.* 270: 19383–90
38. Saurin W, Hofnung M, Dassa E. 1999. *J. Mol. Evol.* 48:22–41
39. Binet R, Letoffe S, Ghigo JM, Delepelaire P, Wandersman C. 1997. *Gene* 192:7–11

40. Salmond GP, Reeves PJ. 1993. *Trends Biochem. Sci.* 18:7–12
41. Koronakis V, Hughes C. 1993. *Semin. Cell Biol.* 4:7–15
42. Dinh T, Paulsen IT, Saier MH Jr. 1994. *J. Bacteriol.* 176:3825–31
43. Paulsen IT, Park JH, Choi PS, Saier MH Jr. 1997. *FEMS Microbiol. Lett.* 156:1–8
44. Koronakis V, Sharff A, Koronakis E, Luisi B, Hughes C. 2000. *Nature* 405: 914–19
45. Andersen C, Koronakis E, Bokma E, Eswaran J, Humphreys D, et al. 2002. *Proc. Natl. Acad. Sci. USA* 99:11103–8
46. Letoffe S, Delepelaire P, Wandersman C. 1996. *EMBO J.* 15:5804–11
47. Thanabalu T, Koronakis E, Hughes C, Koronakis V. 1998. *EMBO J.* 17: 6487–96
48. Holland IB, Benabdelhak H, Young J, Pimenta A, Schmitt L, Blight M. 2003. See Ref. 19, pp. 209–41
49. Havarstein LS, Holo H, Nes IF. 1994. *Microbiology* 140(Pt. 9):2383–89
50. Izadi-Pruneyre N, Wolff N, Redeker V, Wandersman C, Delepierre M, Lecroisey A. 1999. *Eur. J. Biochem.* 261: 562–68
51. Hui D, Morden C, Zhang F, Ling V. 2000. *J. Biol. Chem.* 275:2713–20
52. Michiels J, Dirix G, Vanderleyden J, Xi C. 2001. *Trends Microbiol.* 9:164–68
53. Benabdelhak H, Kiontke S, Horn C, Ernst R, Blight MA, et al. 2003. *J. Mol. Biol.* 327:1169–79
54. Zhang F, Sheps JA, Ling V. 1993. *J. Biol. Chem.* 268:19889–95
55. Delepelaire P, Wandersman C. 1998. *EMBO J.* 17:936–44
56. Palacios JL, Zaror I, Martinez P, Uribe F, Opazo P, et al. 2001. *J. Bacteriol.* 183:1346–58
57. Fernandez LA, de Lorenzo V. 2001. *Mol. Microbiol.* 40:332–46
58. Sapriel G, Wandersman C, Delepelaire P. 2002. *J. Biol. Chem.* 277:6726–32
59. Pimenta AL, Young J, Holland IB, Blight MA. 1999. *Mol. Gen. Genet.* 261:122–32
60. Balakrishnan L, Hughes C, Koronakis V. 2001. *J. Mol. Biol.* 313:501–10
61. Gray L, Mackman N, Nicaud JM, Holland IB. 1986. *Mol. Gen. Genet.* 205: 127–33
62. van Veen HW, Callaghan R, Soceneantu L, Sardini A, Konings WN, Higgins CF. 1998. *Nature* 391:291–95
63. Zhou Z, White KA, Polissi A, Georgopoulos C, Raetz CR. 1998. *J. Biol. Chem.* 273:12466–75
64. Putman M, van Veen HW, Degener JE, Konings WN. 2000. *Mol. Microbiol.* 36:772–73
65. Polissi A, Georgopoulos C. 1996. *Mol. Microbiol.* 20:1221–33
66. Doerrler WT, Reedy MC, Raetz CR. 2001. *J. Biol. Chem.* 276:11461–64
67. Doerrler WT, Raetz CR. 2002. *J. Biol. Chem.* 277:36697–705
68. Reuter G, Janvilisri T, Venter H, Shahi S, Balakrishnan L, van Veen HW. 2003. *J. Biol. Chem.* 278:35193–98
69. Levy SB. 1992. *Antimicrob. Agents Chemother.* 36:695–703
70. Poelarends GJ, Vigano C, Ruysschaert JM, Konings WN. 2003. See Ref. 19, pp. 243–62
71. Ambudkar SV, Dey S, Hrycyna CA, Ramachandra M, Pastan I, Gottesman MM. 1999. *Annu. Rev. Pharmacol. Toxicol.* 39:361–98
72. Zheleznova EE, Markham PN, Neyfakh AA, Brennan RG. 1999. *Cell* 96:353–62
73. Schumacher MA, Miller MC, Grkovic S, Brown MH, Skurray RA, Brennan RG. 2001. *Science* 294:2158–63
74. Yu EW, McDermott G, Zgurskaya HI, Nikaido H, Koshland DE Jr. 2003. *Science* 300:976–80
75. Yu EW, Aires JR, Nikaido H. 2003. *J. Bacteriol.* 185:5657–64
76. Bolhuis H, van Veen HW, Molenaar D, Poolman B, Driessen AJ, Konings WN. 1996. *EMBO J.* 15:4239–45

76a. Shapiro AB, Ling V. 1997. *Eur. J. Biochem.* 250:122–29
77. Margolles A, Putman M, van Veen HW, Konings WN. 1999. *Biochemistry* 38: 16298–306
77a. Ruetz S, Gros P. 1994. *Cell* 77:1071–81
78. Urbatsch IL, Tyndall GA, Tombline G, Senior AE. 2003. *J. Biol. Chem.* 278: 23171–79
79. Yakushi T, Masuda K, Narita S, Matsuyama S, Tokuda H. 2000. *Nat. Cell Biol.* 2:212–18
80. Walker JE, Saraste M, Runswick MJ, Gay NJ. 1982. *EMBO J.* 1:945–51
81. Shyamala V, Baichwal V, Beall E, Ames GFL. 1991. *J. Biol. Chem.* 266: 18714–19
82. Hung LW, Wang IX, Nikaido K, Liu PQ, Ames GFL, Kim SH. 1998. *Nature* 396:703–7
83. Diederichs K, Diez J, Greller G, Muller C, Breed J, et al. 2000. *EMBO J.* 19:5951–61
84. Gaudet R, Wiley DC. 2001. *EMBO J.* 20:4964–72
85. Yuan YR, Blecker S, Martsinkevich O, Millen L, Thomas PJ, Hunt JF. 2001. *J. Biol. Chem.* 276:32313–21
86. Karpowich N, Martsinkevich O, Millen L, Yuan Y, Dai PL, et al. 2001. *Structure* 9:571–86
87. Smith PC, Karpowich N, Millen L, Moody JE, Rosen J, et al. 2002. *Mol. Cell* 10:139–49
88. Schmitt L, Benabdelhak H, Blight MA, Holland IB, Stubbs MT. 2003. *J. Mol. Biol.* 330:333–42
89. Verdon G, Albers SV, Dijkstra BW, Driessen AJ, Thunnissen AM. 2003. *J. Mol. Biol.* 330:343–58
90. Chen J, Lu G, Lin J, Davidson AL, Quiocho FA. 2003. *Mol. Cell* 12:651–61
91. Story RM, Steitz TA. 1992. *Nature* 355:374–76
92. Moody JE, Millen L, Binns D, Hunt JF, Thomas PJ. 2002. *J. Biol. Chem.* 277: 21111–14
93. Davidson AL, Laghaeian SS, Mannering DE. 1996. *J. Biol. Chem.* 271: 4858–63
94. Azzaria M, Schurr E, Gros P. 1989. *Mol. Cell. Biol.* 9:5289–97
95. Al-Shawi MK, Senior AE. 1993. *J. Biol. Chem.* 268:4197–206
96. Loo TW, Clarke DM. 1995. *J. Biol. Chem.* 270:22957–61
97. Davidson AL, Sharma S. 1997. *J. Bacteriol.* 179:5458–64
98. Jones PM, George AM. 1999. *FEMS Microbiol. Lett.* 179:187–202
99. Hopfner KP, Karcher A, Shin DS, Craig L, Arthur LM, et al. 2000. *Cell* 101:789–800
100. Fetsch EE, Davidson AL. 2002. *Proc. Natl. Acad. Sci. USA* 99:9685–90
101. Urbatsch IL, Sankaran B, Bhagat S, Senior AE. 1995. *J. Biol. Chem.* 270: 26956–62
101a. Hrycyna CA, Ramachandra M, Ambudkar SV, Ko YH, Pedersen PL, et al. 1998, *J. Biol. Chem.* 273:16631–34
102. Ferenci T, Boos W, Schwartz M, Szmelcman S. 1977. *Eur. J. Biochem.* 75:187–93
103. Patzlaff JS, van der Heide T, Poolman B. 2003. *J. Biol. Chem.* 278:29546–51
104. Sauna ZE, Ambudkar SV. 2000. *Proc. Natl. Acad. Sci. USA* 97:2515–20
105. Locher KP, Lee AT, Rees DC. 2002. *Science* 296:1091–98
106. Chang G, Roth CB. 2001. *Science* 293: 1793–800
107. Chang G. 2003. *J. Mol. Biol.* 330: 419–30
107b. Mourez M, Hofnung M, Dassa E. 1997. *EMBO J.* 16:3066–77
108. Jones PM, George AM. 2002. *Proc. Natl. Acad. Sci. USA* 99:12639–44
109. Samanta S, Ayvaz T, Reyes M, Shuman HA, Chen J, Davidson AL. 2003. *J. Biol. Chem.* 278:35265–71
110. Mannering DE, Sharma S, Davidson

AL. 2001. *J. Biol. Chem.* 376: 12362–68
111. Hunke S, Mourez M, Jehanno M, Dassa E, Schneider E. 2000. *J. Biol. Chem.* 275:15526–34
112. Nelson SO, Postma PW. 1984. *Eur. J. Biochem.* 139:29–34
113. Reyes M, Shuman HA. 1988. *J. Bacteriol.* 170:4598–602
114. Kuhnau S, Reyes M, Sievertsen A, Shuman HA, Boos W. 1991. *J. Bacteriol.* 173:2180–86
115. Thomas PJ, Hunt JF. 2001. *Nat. Struct. Biol.* 8:920–23
116. Davidson AL. 2002. *Science* 296: 1038–40
117. Campbell JD, Biggin PC, Baaden M, Sansom MS. 2003. *Biochemistry* 42:3666–73
118. Sauna ZE, Muller M, Peng XH, Ambudkar SV. 2002. *Biochemistry* 41:13989–4000
119. Orelle C, Dalmas O, Gros P, Di Pietro A, Jault JM. 2003. *J. Biol. Chem.* 278: 47002–8
120. Janas E, Hofacker M, Chen M, Gompf S, van der Does C, Tampe R. 2003. *J. Biol. Chem.* 278:26862–69
121. Ramachandra M, Ambudkar SV, Chen D, Hrycyna CA, Dey S, et al. 1998. *Biochemistry* 37:5010–19
122. van Veen HW, Margolles A, Muller M, Higgins CF, Konings WN. 2000. *EMBO J.* 19:2503–14
123. Liu R, Sharom FJ. 1996. *Biochemistry* 35:11865–73
124. Grimard V, Vigano C, Margolles A, Wattiez R, van Veen HW, et al. 2001. *Biochemistry* 40:11876–86
125. Vigano C, Grimard V, Margolles A, Goormaghtigh E, van Veen HW, et al. 2002. *FEBS Lett.* 530:197–203
126. Qu Q, Chu JWK, Sharom FJ. 2003. *Biochemistry* 42:1345–53
127. Martin C, Berridge G, Higgins CF, Mistry P, Charlton P, Callaghan R. 2000. *Biochemistry* 39:11901–6
128. Rosenberg MF, Velarde G, Ford RC, Martin C, Berridge G. 2001. *EMBO J.* 20:5615–25
129. Aleksandrov AA, Chang XB, Aleksandrov L, Riordan JR. 2000. *J. Physiol.* 528:259–65
130. Al-Shawi MK, Polar MK, Omote H, Figler RA. 2003. *J. Biol. Chem.* 278: 52629–40

Annual Review of Biochemistry
Volume 73, 2004

CONTENTS